

3rd Trondheim Gas Technology Conference, TGTC-3

Flow pattern transitions in and hysteresis effects of falling film flow over horizontal tubes related to LNG heat exchangers

Anders Austegard^{a*}, Mayukh Bandopadhyay^b, Sigurd Weidemann Løvseth^a, Amy Brunsvold^a

^aSINTEF Energy Research, Trondheim, Norway

^bNorwegian University of Science & Technology, Trondheim, Norway

Abstract

Spiral wound heat exchangers with horizontal tube configurations are used extensively in the chemical, refrigeration, petroleum and food industry, and are core components in many natural gas liquefaction plants. For improved understanding of these heat exchangers, it is of vital importance to predict the liquid flow characteristics between the pipes. In this work, the flow between horizontal tube configurations with different dimensions relevant for LNG heat exchangers was experimentally characterized. N-pentane and methanol were used as test liquids in the experiments. N-pentane has similar properties to LNG and typical mixed refrigerants of LNG processes. The new experimental results were compared with existing models and other literature data.

© 2015 Published by Elsevier Ltd. This is an open access article under the CC BY-NC-ND license

(<http://creativecommons.org/licenses/by-nc-nd/4.0/>).

Peer-review under responsibility of the Scientific Committee of TGTC-3

Keywords: Droplet; Column; Jet; Sheet; Flow pattern; hysteresis; tubes

1. Introduction

The use and transportation of LNG has seen a rapid increase over the last decades. This growth is posed to continue in the decades ahead, in accordance to for instance the IEA 450 (2 °C) scenario [2], and a large number of LNG carriers are under order.

Although LNG is the most efficient way of transporting natural gas over longer distances, the liquefaction process is still costly in terms of investments and energy consumption. The heat exchangers are central to any liquefaction process, and a detailed understanding of their operation is hence key to improve the LNG production further in terms of efficiency, cost, and process robustness. In the last heat exchanger step of LNG processes, the

* Corresponding author. Email: Anders.Austegard@sintef.no

natural gas is partially or fully liquefied. In most processes of commercial interest, the low-pressure refrigerants are evaporated within the heat exchangers, whereas one or more high pressure refrigerants are cooled with the natural gas and liquefied. Hence, insight into LNG heat exchanger operation requires understanding of a coupled problem involving thermodynamics, heat transfer, and multi-phase flow.

The dominating heat exchanger types in LNG plants are spiral wound and plate fin heat exchangers. SINTEF Energy Research is currently investigating flow phenomena related to the former, often called coil-wound heat exchangers, which are used for instance in the well-established APCI C3/MR process and the newer Linde/Statoil MFC-process. These heat exchangers consist of multiple coils wound helically around a center mandrel. In natural gas liquefaction plants, the heat exchanger is placed up-right such that the tubes are almost horizontally oriented. The distances between neighboring tubes are relatively short. During operation, there will be a falling film, typically of the low pressure refrigerant, on the surface of and between the tubes. Similar falling film heat exchangers with horizontal tube configuration have widespread application in the chemical, refrigeration, petroleum and food industry. These heat exchangers operate with high heat transfer coefficient and small liquid inventory. The local heat transfer between the tube and the shell side fluids depends on the falling film characteristics, like the film thickness, flow pattern, and the stability of the film on the tubes, resulting from the pattern of the falling film between the tubes. For instance, on tube surfaces without liquid film the heat transfer will drop significantly.

However, a main challenge involved in designing these heat exchangers is the absence of an empirical model that can be used for predicting the falling film flow patterns. Improving the fundamental understanding of the two phase flow phenomena is imperative for the development of advanced models, which in turn can provide an improved basis for designing and operating cryogenic heat exchangers. A critical literature review [1] revealed that there is insufficient information about flow pattern transitions for dimensions and fluids relevant for LNG spiral wound heat exchangers, characterized for instance by the relatively short distance between the tubes and low viscosity and surface tension of the liquid.

The main focus of the work to be presented in this paper was to analyze the flow pattern transitions of falling flow over a vertical array of horizontally positioned tubes, which constitutes a good starting point to study these effects with a limited number of variables in order to get meaningful results. Emphasis was laid on identifying the flow pattern transitions and relating the transitions to dimensionless parameters. In the experiments, n-pentane was used as model liquid since its fluid properties are close to mixed refrigerants used in LNG processes [3].

2. Relevant flow regimes and flow transition models

2.1. Flow patterns

Falling film flow can be classified in a range of different ways. Most of the literature we have studied refers to three main flow patterns, which are illustrated in Figure 1: Droplet (D), column (C), sometimes called jet, and sheet (S) flow. By including the intermediate flow states between these patterns, there are in total 5 flow regimes that can be identified. Some authors, like Wang [4], operate with eight flow regimes by using additional intermediate states. In some works, e.g. Hu [5], also staggered and inline column patterns are included.

In Figure 2, images from our lab of the different flow regimes and intermediate states are shown. With increasing flow rates, the flow pattern changes from droplet, via column, to sheet flow. In the images shown in

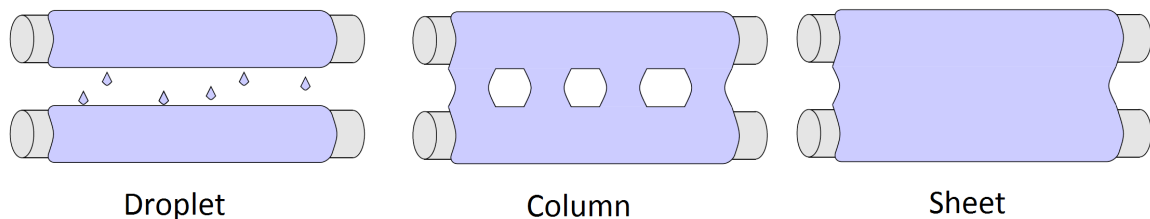


Figure 1: Illustration of the main relevant flow regimes, from Zhao [1]

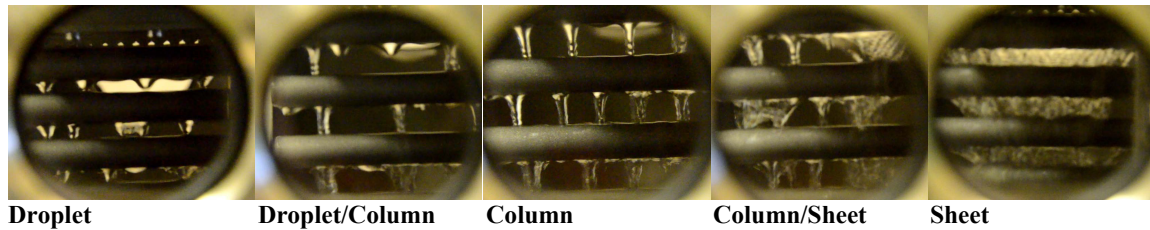


Figure 2: Photo of flow regimes how it looks with N-pentane with 8mm tubes.

Figure 2 it can clearly be seen that for the intermediate states, two "pure" flow patterns are coexisting at the same time but at different locations. Sometimes a flow regime is stable, but the patterns can also be unstable, for instance the columns could be moving back and forth. In this paper, we will denote the transitional state between droplet and column for Droplet/Column (DC), and the transitional state between column and sheet Column/Sheet (CS).

Some energy is required in order to go from one flow regime to another, for example to break up a sheet as the flow decreases. Like in most physical systems, such an energy barrier will cause hysteresis [5], meaning for instance that it is expected that the transition from column to sheet flow occurs at a higher flow than the reverse transition.

2.2. Models for flow regime transitions

This particular flow problem can be characterized by the parameters listed in Table 1. Three of the parameters, ρ_L , μ_L , and σ , are characteristics of the fluid; D , S , and k characterize the tube array; whereas Γ and g are the other parameters affecting the flow. The contact angle θ is not assumed to have any influence since the complete tube surface with flow is wet during the experiments. Sand blasted steel tubes are used. The maximum Reynolds number is below 1200 and the film is laminar. The roughness k is small compared with the thickness of a laminar film; hence, it is assumed the roughness is of minor importance. A spiral wound heat exchanger is typically made of aluminum tubing. Aluminum has different contact angle θ and can have different roughness. But except at very rough surfaces, neither roughness or contact angle or any other differences between aluminum and steel are expected to influence the flow regime to a significant degree.

Table 1: Flow problem model input parameters.

Symbol	Description	Unit	Symbol	Description	Unit
ρ_L	Liquid density	kg/m ³	S	Tube separation	m
μ_L	Liquid viscosity	Ns/m ²	k	Surface roughness	m
σ	Surface tension	N/m	Γ	Mass flow/flow width	kg/(m·s)
D	Tube diameter	m	g	Acceleration of gravity	m/s ²

From these parameters shown in Table 1 common dimensionless numbers can be constructed, e.g.:

$$Re = \frac{2\Gamma}{\mu_L}, \quad Ga = \frac{\rho_L \sigma^3}{\mu_L^4 g} = \left(\frac{g(Ca)^3 \rho}{\mu^2} \right)^2, \quad \frac{S}{Ca} \quad (1)$$

Here Re and Ga are the Reynolds and modified Galileo[†] numbers of the flow problem and Ca is the capillary length:

[†] After Galileo Galilei, hence sometimes called Galilei number

$$Ca = \sqrt{\sigma / (\rho g)} \quad (2)$$

The Reynolds number (Re) is the inertia forces divided by the viscous forces. The capillary length Ca is a characteristic length scale for a surface between two fluids affected by gravitation and surface tension. The modified Galileo number (Ga) [5] is often called the Kapica number (Ka) [6]. With gravitation given, Ga is a function of the fluid properties and dependent on the relation between surface tension and viscosity. The ordinary Galileo number equals the inertial forces times gravitational forces divided by the square of the viscous forces. Ga is the square of the ordinary Galileo number based on a capillary length scale Ca .

For convenience a new dimensionless parameter Y is defined as:

$$Y = \frac{Re}{Ga^{1/4}} = \frac{2\Gamma g^{1/4}}{\rho_L^{1/4} \sigma^{3/4}} = \frac{2\Gamma}{\sigma^{1/2} Ca^{1/2}} \quad (3)$$

Y is independent of liquid viscosity and is the square root of the ratio between the inertial force and gravitational force based on a length scale of the capillary length Ca .

In the literature, dimensionless empirical models for the transition between flow regimes involving Re and Ga are often fitted to experiments. All references found and discussed later in this work fit the parameters of the following equation to the flow transitions:

$$Re = a \times Ga^b \quad (4)$$

a and b are constants specific to a flow regime transition. Some authors set $b = 1/4$, meaning $Y = Re/Ga^{1/4}$ is constant and equal to a , and in all cases found in the literature b is close to $1/4$. Setting $b = 1/4$ is a convenient choice used in this work which makes Y constant and the transition independent of the viscosity. Jacobi [7] used a slightly more advanced model:

$$Re = a \times Ga^{1/4} \sqrt{S/Ca} \quad (5)$$

Hence, in Jacobi's model the transitions occur at higher Reynolds number for longer distances between the tubes. The assumption is that the prevalent flow pattern is the one with minimum energy, which means that the surface area of the flow should be minimized. Further, it was assumed that the distances between the columns are equal to $2\pi\sqrt{3} \times Ca$, and that the droplet diameter is $3Ca$.

2.3. Simplification compared to a real heat exchanger

The tubes in a real heat exchanger are not horizontal but somewhat inclined. Further, the tubes are supported regularly. Hence, in the droplet flow regime it is expected that some of the liquid follows the underside of the tube until a support is reached and the liquid flows to the next tube. This phenomenon should be less prevalent for column or sheet flow. In order to limit the number of parameters in this initial study, horizontal tubes are used. Axial flow due to inclined heat exchanger tubes should be studied separately.

In a real heat exchanger there may also be non-zero vapor flow velocity, which has been studied by Ruan [8] and shown to have a considerable effect. In this work, the flow regime is studied with practically no flow outside of the tubes.

3. Experimental setup and procedures

3.1. Fluids

The liquids under test are n-pentane and methanol with 99.0% and 99.9% purity, respectively. Relevant properties of the liquids are shown in Table 2. As can be seen from the table, n-pentane is a fairly good match to liquid methane. In a thorough review of these properties, Zhao et al. [3] showed that the match between n-pentane and relevant mixed refrigerants was even better over a large temperature span. Hence, n-pentane is a suitable model liquid for investigation of LNG heat exchanger flow phenomena. N-pentane has low surface tension and low viscosity.

Table 2 Properties of different fluids investigated here and in the literature

Liquid	At temperature (°C)	ρ_L kg/m ³	σ mN/m	μ_L mN/m ² s	$Ga^{1/4}$	Ca mm	Source
N-pentane	40	606	13.7	0.197	569	1.52	Fröba, Kröner [9, 10]
Methanol	20	792	22.5	0.583	294	1.70	NIST [11]
Liquid methane	-162	422	12.9	0.112	875	1.77	NIST [11]
Water	20	998	72	1.0	441	2.71	NIST [11]

3.2. Setup

The experimental setup is illustrated in Figure 3 with a principal sketch of the whole setup shown to the left and an image of the tube array simulating what is found in a spiral wound heat exchanger below a drip-hole arrangement to the right. Inside the **experimental chamber** there are two liquid **reservoirs**, one at the bottom of the chamber and

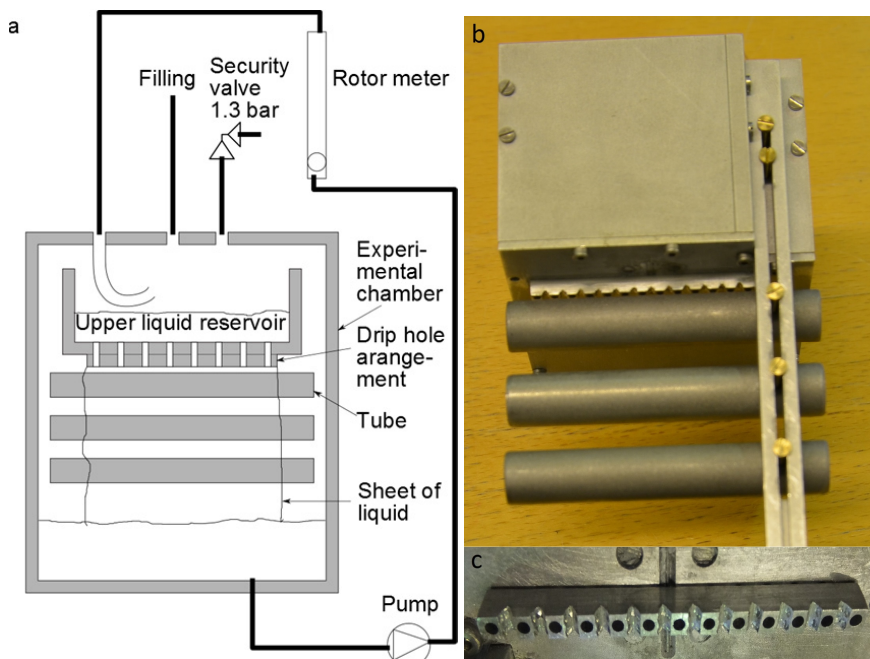


Figure 3: Experimental setup: (a) Schematic drawing, (b) tube array with upper cup, (c) drip holes

one in a cup above the drip-hole arrangement. After filling the chamber with the fluid under study, liquids are pumped from the bottom of the chamber to the upper cup by using an external circuit. The upper cup is drained by an array of holes at its bottom, called the **drip-hole arrangement**, shown at the bottom of Figure 3. The 1.6 mm diameter holes are drilled at an interval of 4 mm, resulting in an effective array length of $L=52$ mm.

The drip holes are placed directly above an array of 3 or 4 horizontal and identical

tubes, each with a length of 70 mm. In the current study, tubes with diameters of $D = 8$ mm and $D = 12$ mm were used. The tubes are sand blasted, resulting in a surface roughness of approximately $k \approx 0.02$ mm. The tubes are mounted on a vertical straight bracket as seen in Figure 3, and the tubes can be moved up and down the bracket such that their separation S can be adjusted. In this work, S was set to 3, 4, 6 or 8 mm. Note that S is defined as the separation between the tubes, such that the tubes are mounted at an interval of $S+D$.

In our experiments, the distance between columns during column flow is around 14 mm. The distance between points of droplet formation under the tubes is similar. Hence, it is assumed that the drip-hole interval of 4 mm is short enough to create a close to uniform flow across the pipe.

The pressure during the experiments is between 1.0 and 1.2 bar absolute measured using a sensor inside the experimental chamber. The temperature is adjusted to 37 ± 2 °C and 20 °C ± 2 °C during the experiments with n-pentane and methanol, respectively, with uncertainty given with 95 % confidence. The temperature is measured and controlled using two thermoelements inside the chamber and a heater using water as heating medium. The chamber is always run with equilibrium vapor concentration; hence, there is no dry-out of the tubes. A frequency controlled positive volume displacement type **pump** with frequency from 3 to 25 Hz is used to regulate the flow. The flow rate of the pump is calibrated by measuring the time it takes to fill a cup of 449 cm³ at different pump frequencies. In addition, a **rotor meter** is used as an extra control of the flow rate in some experiments. The upper reservoir serves as an integrating element in the liquid flow circuit, and if there were any pulsations of the flow from the pump, these are not observable in the flow from the drip-hole arrangement or across the tubes.

The experimental chamber is equipped with windows enabling visual inspection and capture of the dynamic flow patterns using a camera, as seen for instance in Figure 2 with S equal to 6 and 8 mm. For smaller tube separations S it is more difficult to identify the flow regimes.

3.3. Experimental procedure

The hysteresis is very dependent on how the experiments are performed. When the flow is increasing fast there will typically be large hysteresis, but the effect will be smaller for instance if flow pattern changes are induced by disturbance or with slower changes in flow rates.

For each configuration in our work, the pump frequency is increased from 3 to 25 Hz giving a flow from 0.4 to 3 cm³/s, and then lowered back again to 3 Hz such that hysteresis effects may be quantified. The flow is incremented or decreased in steps of 0.05 cm³/s or less. At each step, the pump has been running for at least 15 seconds before the flow stabilizes.

4. Results

4.1. Uncertainty of measurements

Before any conclusions can be made from the experiments, the uncertainty in the estimation of model parameters must be found, following commonly accepted principles [12]. The objective of the experiments is to quantify at which values of Y the different flow regime transitions occur.

From equation (3) it can be seen that:

$$Y = Y(Q, \rho_L, g, L, \sigma) = \frac{Re}{Ga^{1/4}} = \frac{2Q\rho_L^{3/4}g^{1/4}}{L\sigma^{3/4}}, \quad \frac{\partial Y}{\partial Q} = \frac{Y}{Q}, \quad \frac{\partial Y}{\partial L} = -\frac{Y}{L} \quad (6)$$

Here $Q = L\Gamma / \rho_L$ is the volume flow. The uncertainty in g is assumed to be insignificant. The physical properties σ and ρ_L is well known for pentane, and analysis has shown that the uncertainty is low compared other uncertainties. Then the only remaining parameters in (6) are Q and L .

The flow Q is given by the frequency of a positive displacement pump. The flow as a function of pump frequency is calibrated by measuring the time to fill a container with volume 449.6 cm³. Based on the spread in the calibration the repeatability of Q was quantified in terms of a standard deviation of 0.29 cm³/s, corresponding to a standard

deviation of 0.062 in Y . The associated contribution to the expanded uncertainty with 95 % confidence is two times the standard deviation. Further, the flow transitions are not always clearly identifiable, causing additional uncertainty in Y . The transitions are most difficult to detect when the tubes are close to each other, i.e. when S is low. The repeatability in detecting the flow transitions was estimated for two cases, and the standard deviation was estimated to be 0.04 in Y . This was in fact smaller than the estimated uncertainty for the flow fluctuations which it should include.

Estimating L is not straight forward, it is not necessary equal to the width of the drip hole array. As seen in Figure 2, the surface tension reduces the width L of the films as they are falling, whereas L is increasing when the flow passes the tubes. It is assumed that the effect of the surface tension is largest at both edges of the sheet. The corresponding uncertainty in Y is estimated to be 15% and this is a systematic error.

4.2. Comparison between experiment and real LNG heat exchangers

In Section 4.1 we discussed the uncertainty in identifying Y corresponding to flow regime transitions in our setup. The value of the measurements is however also dependent on how well they represent real heat exchanger flow. In addition, the energy barriers between the flow regimes cause hysteresis, as discussed in Section 2.1 and 3.3. In a real heat coil-wound LNG heat exchanger the length of the tubes is large; there are many tubes, and no hysteresis. In the experimental setup we are using a few tubes with finite length, and hysteresis is present since we keep each flow rate a limited length of time.

The deviation caused by hysteresis seems rather arbitrary and depends on factors such as the level of mechanical disturbances and the duration of which the flow rate is kept constant. Because we see a large variation in the hysteresis, the hysteresis is included in the uncertainty calculation.

We also see a difference in the value of Y at the transitions between the tubes of the array. When four tubes are used, the transitions occur first between tube 3 and 4 (lower tube pair), then between tube 2 and 3, and finally between tube 1 and 2 (upper tube pair). As can be observed in Figure 2 and discussed in Section 4.1, the surface tension tend to concentrate the flow as it progresses downward, giving an effective higher flow rate per length, especially at the edges during sheet flow, which may explain these differences in the transition flow rate. On the other hand, the flow at the lower pipes is more turbulent which should move the transition in the opposite direction. The average value of the tube array has the best repeatability and is reported in this work.

The uncertainty in Y caused by hysteresis and differences between the different falling flows in the experiment are summarized in Table 3. For simplicity and in lack of large amounts of data, the uncertainty is averaged over all measurements. As can be seen, these terms are dominating compared with the other terms discussed above, resulting in a total compounded standard uncertainty of $u_Y = 0.17$, corresponding to a 95 % confidence interval of Y of ± 0.34 .

Table 3 Estimation of difference from an ideal case

Source of uncertainty and its estimation	Contribution to standard uncertainty in Y , u_Y
Difference from average of all cylinders and an ideal case, estimated by averaging the difference between first and third cylinder for when transition happen for all experiments with 4 cylinders.	0.11
Hysteresis: Difference in transition value between increasing and falling flow rates averaged over all measurements	0.093

4.3. Measurements and model fitting

In Figure 4, the measured values of Y as defined by equation (3) for the different transitions between the 5 flow regimes are shown for a selection of tube separations S and diameters. Most of the experiments are done with n-pentane, but also methanol was investigated. The measurements are shown separately for increasing and decreasing flow. Hence, hysteresis is evident, but in a few cases the difference is opposite of what is expected, probably due to inaccuracies in the measurements. For reference, estimated contribution from repeatability to the expanded

uncertainty, i.e. 95 % confidence and $k=2$, is shown in the upper left plot. The average value of Y for pentane is shown for each tube diameter and transition using solid lines. The average RMS difference between the measured points and these average values is 0.16.

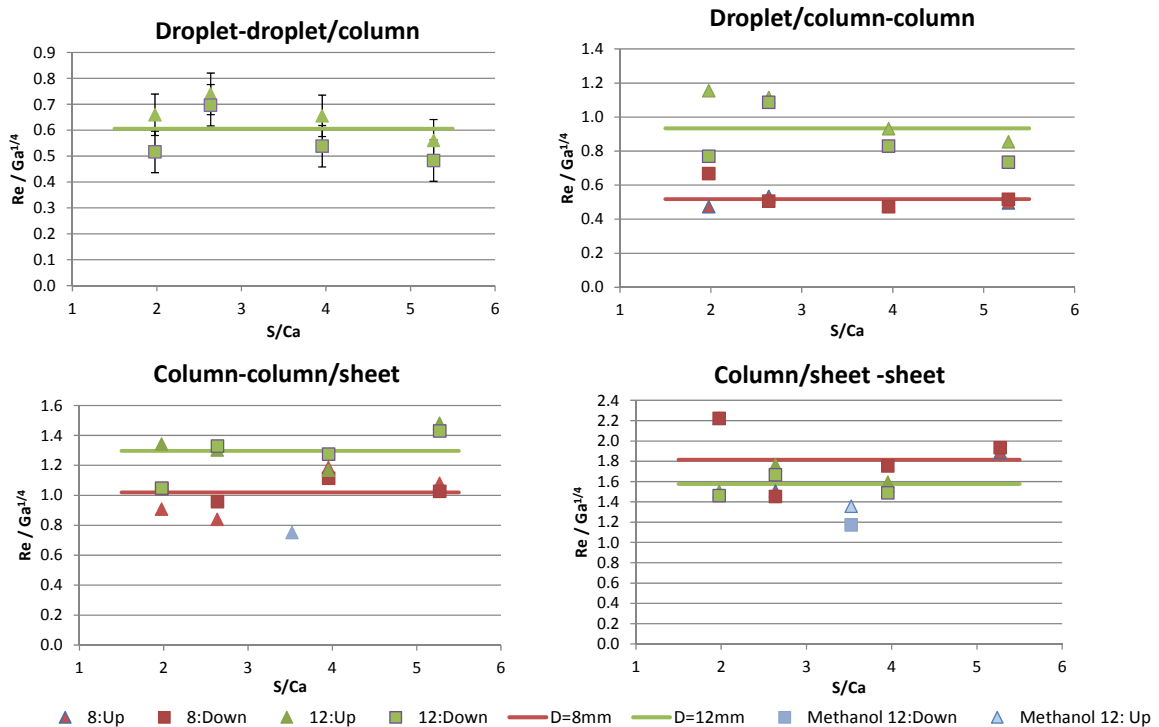


Figure 4 : Measured values of Y as defined by equation (3) for the different transitions between the 5 flow types for n-pentane and methanol

In Figure 5, the measured values of Y for each transition averaged over tube diameters and hysteresis effects are plotted as a function of tube separation S . No systematic dependence on S is seen. The RMS difference from the measured points to the average value for each transition is 0.23. This might be expected since the empirical model employed does not take into account the diameter of the tubes, which certainly is expected to have some impact with diameters comparable to the tube separations. Note that the RMS difference between the plotted points and the lines in Figure 5 is smaller since the plotted points are already averaged. The model given by equation (5) is indicated with dashed lines, but our data does not support such a dependence on tube separation S and the base model (4) is more suitable.

5. Comparison with literature data

In Figure 6, literature data on flow regime transitions models are shown and compared with our recent measurements. What is plotted is the parameter Y for n-pentane. All literature sources have been using the model given by equation (4), with different estimates for parameters a and b . All previously reported studies except Honda [13] have been using water or other fluids with high surface tension and viscosity. Honda reported similar flow regime transition values of Y as the current work using low-finned tubes and n-pentane. Hu and Jacobi [5] have done experiment with the similar dimensionless parameters (Re , Ga , S/Ca and D/Ca) as this work, using water at high temperature with larger tubes, and got different results. Otherwise, the values we have measured for Y for n-pentane is higher than the values reported for other liquids in the literature, whereas methanol is at the same level. Generally,

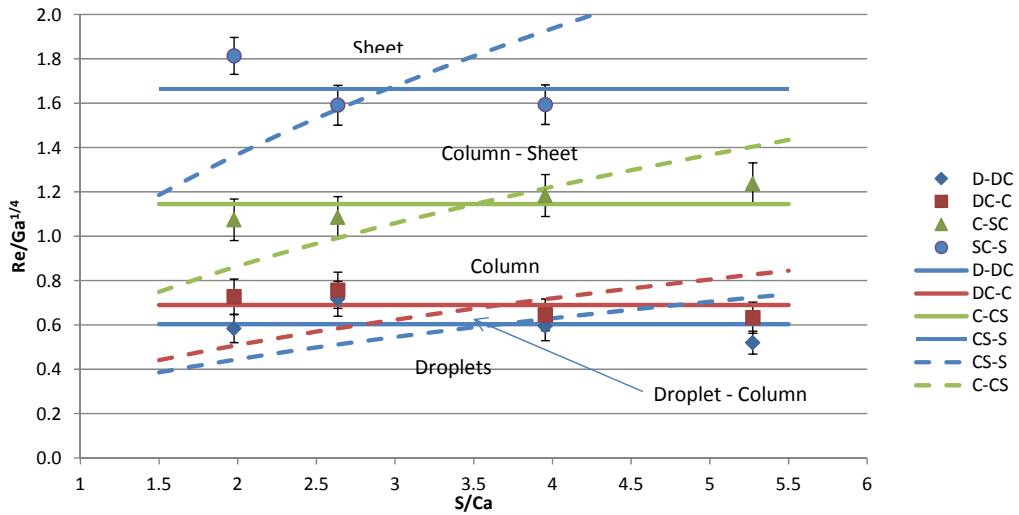


Figure 5: The same transitions as in Figure 4 averaged over hysteresis effects and tube diameter. Dashed lines show the fitting to equation (5).

the other studies have longer distances between the tubes and hence less relevant for LNG coil-wound heat exchangers.

Compared with some other the literature data, our work has a relative broad range Y -values with column/sheet flow. The width of this flow regime is probably related to the measurement uncertainty and changes with experimental setup and subjective criteria for the characterization of the flow regime.

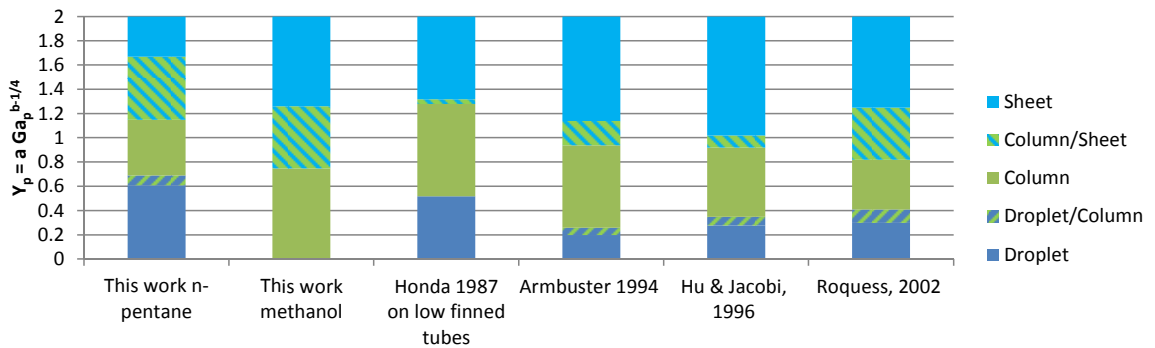


Figure 6: Comparison of Y_p -value for n-pentane (Y_p) between this work and corresponding estimates from literature models [5, 13-15] for n-pentane at 40°C where $Ga_p = 1.0482 \times 10^{11}$. The transitions from column flow to droplet or droplet/column is not measured for methanol. All literature uses equation (4) with $Re = a \times Ga^b \Rightarrow Y = Re / Ga^{1/4} = a \times Ga^{b-1/4}$. The literature values for b are shown in Table 4.

Table 4 The exponent b in equation (4) from relevant literature when different from 1/4. The value of a can be calculated from Figure 6.

	Droplet ↔ Droplet/Column	Droplet/Column ↔ Column	Column ↔ Column/Sheet	Column/Sheet ↔ Sheet
Honda 1987 [13]	0.25	0.25	0.25	0.236
Hu & Jacobi, 1996 [5]	0.30	0.30	0.23	0.24
Roques, 2002 [15]	0.33	0.32	0.25	0.26

6. Conclusions

Spiral-wound heat exchangers are vital parts of many LNG plants, and a thorough understanding of flow phenomena inside them is needed for improved design and operation. In this work, the falling film behavior around a tube array simulating typical spiral wound heat exchanger configurations has been investigated using n-pentane, which has properties similar to mixed refrigerant liquids in LNG plants, and methanol. The transitions between different flow regimes, droplets, column, sheet, and hybrids between them have been characterized for different spaces between and diameters of tubes. The measurements were analyzed in terms of empirical models using dimensionless numbers like the modified Galileo and Reynolds numbers employed elsewhere in the literature. Our results indicate that these empirical models are not universal and appropriate when applied to liquids with significantly different properties and closely spaced tubes. More experiments, with longer and higher number of tubes, should be performed to develop more accurate correlations. These can later be extended by studying the effects of tilt and vapor flow.

7. Acknowledgements

This publication is based on results from the research project *Enabling low emission LNG systems*, performed under the PETROMAKS 2 program. The authors acknowledge the project partners, Statoil and GDF SUEZ, and the Research Council of Norway (193062/S60) for support. The authors also would like to thank Jostein Pettersen for valuable input and discussions.

References

- [1] Zhao H, Aursand P. Internal report, Enabling Low-Emission LNG Systems project. 2012.
- [2] *World Energy Outlook 2013*, International Energy Agency, Paris, France; 2013.
- [3] Zhao H, Brunsvold A, Munkejord S, Mølnevik MJ. An experimental method for studying the discrete droplet impact phenomena in a flammable gas environment. *Journal of Natural Gas Science and Engineering*; 2010;2:259-69.
- [4] Wang X, Hrnjak PS, Elbel S, Jacobi MA, He M, "Flow Pattern and Mode Transitions for Falling Film on Flat Tubes," in *International Refrigeration and Air Conditioning*, Purdue University; 2010.
- [5] Hu X, Jacobi MA. The intertube falling film, part 1 - flow characteristics, mode transitions and hysteresis. *Journal of heat transfer*; 1996;118:626-33.
- [6] Kunes J, *Dimensionless Physical Quantities in Science and Engineering*. Elsevier Science; 2012.
- [7] Jacobi MA, Wang X, "A Thermodynamic Basis for Predicting Falling Film Mode Transitions," in *International Refrigeration and Air Condition Conference*, Purdue University; 2012.
- [8] Ruan B, Jacobi MA, Li L, "Vapour Shear Effect on Falling-Film Mode Transitions Between Horizontal Tubes," in *International Refrigeration and Air Condition Conference*, p. 1-8, Purdue, Indiana, USA; 2008.
- [9] Fröba AP, Penedo Pellegrino L, Leipertz A, "Viscosity and surface tension of saturated n-pentane," in *15th Symposium on Thermophysical Properties*; 2003.
- [10] Kröner A. An Engineering Company's Approach to Filling "CAPE Gaps" in Process Simulation. In *Proceedings of 16th European Symposium on Computer Aided Process Engineering and 9th International Symposium on Process Systems Engineering*, 2006, *Computer Aided Chemical Engineering*; 2006; 21, Part 1: 781-6.
- [11] "Thermophysical Properties of Fluid Systems," <http://webbook.nist.gov/>.
- [12] Taylor BN, Kuyatt CE, *Guidelines for Evaluating and Expressing the Uncertainty of NIST Measurement Results*, NIST Technical Note, vol. 1297, 1994 edition, Gaithersburg, Maryland, USA; 1994.
- [13] Honda H, Nozu S, Takeda Y, "Flow characteristics of condensation on a vertical column of horizontal low finned tubes," in *ASME-JSMA Thermal Engineering Joint Conf.*, p. 517-24, Honolulu, HI; 1987.
- [14] Armbuster R, Mitrovic J, "Patterns of falling film flow over horizontal smooth tubes," in *Proc. 10th Int. Heat Transfer Conf.*, p. 275 - 80, Brighton, UK; 1994.
- [15] Roques J-F, Thome JR. Falling Film Transitions between Droplet, Column, and Sheet Flow Modes on a Vertical Array of Horizontal 19 FPI and 40 FPI Low-Finned Tubes. *Heat Transfer Engineering*; 2003;24:40-5.